THE ASTROPHYSICAL JOURNAL, 209:452–461, 1976 October 15

A DENSE MOLECULAR CLOUD IN THE OMC-1/OMC-2 REGION

MARC L. KUTNER
Goddard Institute for Space Studies; and Department of Physics, Rensselaer Polytechnic Institute
NEAL J. EVANS II
Owens Valley Radio Observatory, California Institute of Technology; and
Department of Astronomy, University of Texas, Austin
AND
KENNETH D. TUCKER
Department of Physics, Fordham University
Received 1975 December 19; revised 1976 March 26

ABSTRACT

H_2CO emission at 2 mm is seen over a region 30′ in extent which includes OMC-1 and OMC-2. The mass of this cloud, estimated from H_2CO and CO observations, is $\sim 7 \times 10^3\ M_\odot$. The velocity pattern is one of rotation, with evidence for fragmentation into two or three distinct condensations. A sharp boundary to the molecular cloud is observed at the edge of the H II region in NGC 1977. It appears likely that NGC 1977 is a condensation at the northern end of the cloud, complementary to the Orion Nebula at the southern end.

Subject headings: interstellar: molecules — nebulae: general

I. INTRODUCTION

The molecular cloud associated with the Kleinmann-Low nebula has been studied by means of many molecular transitions at centimeter and millimeter wavelengths. This cloud, referred to as OMC-1, is the strongest known source of millimeter-wave emission from a number of molecules. The thermal structure of OMC-1 and its environs, as determined from observations of the $\lambda = 2.6$ mm transition of carbon monoxide (CO), has been extensively mapped. A hot core of CO emission, centered on the Kleinmann-Low nebula, lies within a 30′ long, essentially north-south, plateau from which CO emission of ≥ 30 K is observed (Liszt 1974; Kutner *et al.* 1976). Surrounding and apparently containing the plateau is the diffuse dust cloud Lynds 1641 (Lynds 1962), from which CO emission has been observed over an area of ~ 18 square degrees (Kutner *et al.* 1976).

A comparably complete picture of the density structure of the Orion region is only now beginning to emerge. The densest region ($n_{H_2} \geq 10^6\ cm^{-3}$) is less than 1′ across and is probably directly associated with the infrared nebula (see, e.g., Kutner *et al.* 1973). This core is surrounded by an area of slightly lower density ($n_{H_2} \approx 10^5\ cm^{-3}$), with a north-south extent of $\sim 5'$ and slightly less east-west extent (Thaddeus *et al.* 1971; Harvey *et al.* 1974; Evans *et al.* 1975). Recent 1 mm continuum and 2 cm formaldehyde (H_2CO) emission maps have revealed an extension of this region to the north and northeast (Harvey *et al.* 1974). A new molecular and infrared source, designated OMC-2 (Gatley *et al.* 1974), has been found 12′ north and 3′ east of OMC-1. Millimeter emission from hydrogen cyanide (HCN), observed in the direction of OMC-2 by Morris *et al.* (1974) shows a north-south elongation.

In this paper we present detailed observations of carbon monoxide at $\lambda = 2.6$ mm and formaldehyde at $\lambda = 2$ mm and 2 cm in the region of the sky containing the two Orion molecular sources. These observations reveal an extremely long, dense molecular cloud, extending from OMC-1 to OMC-2 and then another quarter of a degree to the north and northwest.

II. OBSERVATIONS

The millimeter-wave observations were made in 1974 December with the 16 foot (5 m) antenna of the Millimeter Wave Observatory, Fort Davis, Texas.[1] The half-power beamwidth is 2′.6 at 2.6 mm and 2′ at 2 mm. Spectral resolution of 250 kHz (0.5 km s^{-1} at 2 mm) was provided by a 40 channel filter bank. Baseline stability was achieved by frequency switching at 5 Hz. Calibration was done using an absorbing chopper wheel in front of the feed. The scale of radiation temperatures ($T_R = I_\nu \lambda^2/2k$), corrected for atmospheric attenuation and beam efficiency, was established in the manner of Davis and Vanden Bout (1973), with a slight modification to account for the different atmospheric distributions of oxygen and water vapor.

Observations of the 2_{11}–2_{12} (2 cm) transition of H_2CO at 14.4 GHz were made in 1975 October with the National Radio Astronomy Observatory[2] 140 foot

[1] The Millimeter Wave Observatory is operated by the Electrical Engineering Research Laboratory, the University of Texas at Austin, with support from the National Aeronautics and Space Administration, the National Science Foundation, and McDonald Observatory.

[2] Operated by Associated Universities, Inc., under contract to the National Science Foundation.

(43 m) telescope. The 384 channel autocorrelator provided spectral resolution of 0.135 km s^{-1}. Observations were made with frequency switching of the first local oscillator, and data from two orthogonal polarizations, observed simultaneously, were averaged together. Observations of the full Moon and Jupiter indicated a beam efficiency of 67 percent for an extended source and 42 percent for a 45″ diameter source. A noise tube was used for calibration, and correction for atmospheric attenuation was made by noting the contribution to the system noise temperature made by the sky. The antenna temperature of the emission line in the direction of the KL nebula agrees with the value of 0.45 K found by Zuckerman and Evans (unpublished).

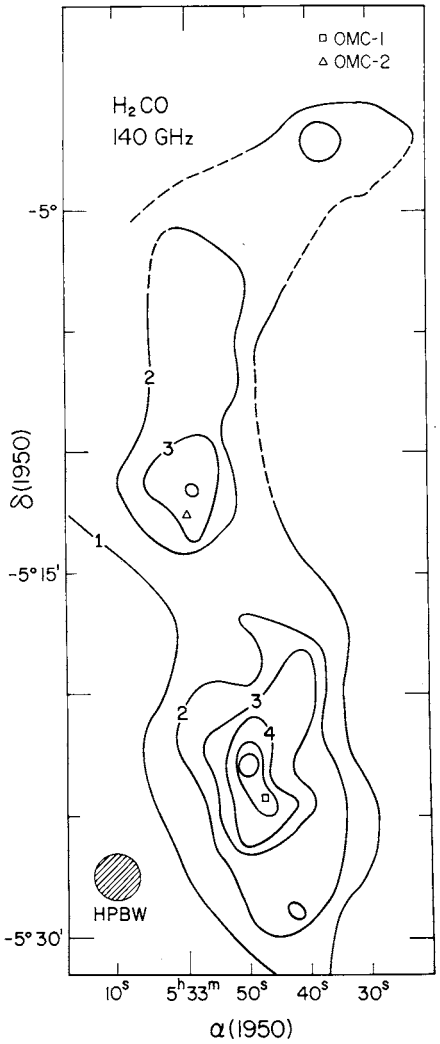

FIG. 1.—Two millimeter formaldehyde emission from the OMC-1/OMC-2 region. The contours are of peak radiation temperature of the 140 GHz line. The map was sampled at one beamwidth intervals (indicated by the shaded circle) over most of the region, and half-beamwidth intervals in the vicinity of peaks. The dotted lines indicate regions where the H_2CO emission may extend beyond the area studied.

a) H_2CO

A map of the $2_{12} \rightarrow 1_{11}$ line of H_2CO at 140.8 GHz is presented in Figure 1, which shows the peak line radiation temperature as a function of position. Emission at a level greater than 1 K is seen over a north-south extent of greater than half a degree and an east-west extent of about 8′. Our map does not reach the eastern boundary of the 1 K emission in the northern part of the cloud. Two emission peaks associated with OMC-1 and OMC-2 are clearly defined, though in neither case does the peak line radiation temperature occur at the position of the corresponding infrared source. In OMC-1, the actual maximum radiation temperature occurs slightly to the northeast of the KL nebula; but since the line in this direction is narrow, the line in the direction of KL has the greater integrated intensity. Similar behavior has been observed in maps of C_2H (Tucker and Kutner 1976) and CN (Turner and Gammon 1975). The second H_2CO peak is 1′ north of OMC-2. The formaldehyde linewidth in the direction of OMC-2 is 1.7 km s^{-1}, the same as for HCN (Morris *et al.* 1974). Each peak is surrounded by an extended ($\sim$10′ long) source of >2 K H_2CO emission. The linewidth over most of this region is about 1.5 km s^{-1}.

In addition to mapping the normal isotopic species of formaldehyde, we have also observed the $2_{12} \rightarrow 1_{11}$ transition in the isotopically substituted species $H_2{}^{13}CO$ at 137.4 GHz. The profiles for both isotopes in the direction of OMC-1 are shown in Figure 2. The intensities of both of these lines are in agreement with those found by Wannier *et al.* (1976), but our $H_2{}^{13}CO$ line was half the width of that found by Wannier *et al.*

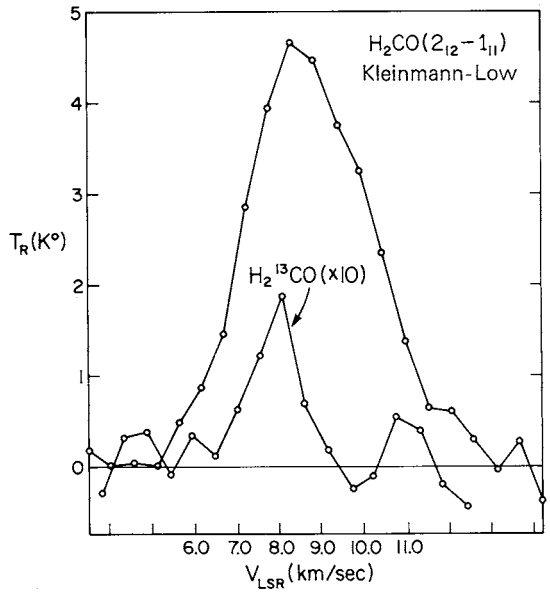

FIG. 2.—Two millimeter formaldehyde spectra in the direction of the Kleinmann-Low nebula. The top curve is the 140 GHz line, and the lower curve is the corresponding transition in $H_2{}^{13}CO$, with the intensity multiplied by a factor of 10.

Given the noise level in both measurements, it is probable that both results are consistent with an intermediate value. We have also obtained an upper limit of 0.2 K for the $H_2{}^{13}CO$ line in the direction of the peak northeast of OMC-1.

The 2 cm observations were made to allow us to analyze the 2 mm data in terms of densities of hydrogen and formaldehyde. Possible weak ($T_R \approx 0.05$ K) absorption lines appeared at two positions, 3′ and 6′ north of OMC-2. In the direction of OMC-2 and 1′ north, 0.05 K emission lines were observed. No emission or absorption was detected elsewhere in a grid of positions spaced by 2′–3′ and running along the peak of the 140.8 GHz emission region from $-5°20'$ to $-4°57'$. Points were spaced more closely around OMC-2, and a point 3′ east of the emission peak was observed at $-5°05'$. Upper limits were established by taking half the peak-to-peak noise and dividing by an efficiency of 0.4, which allows for lower efficiency at lower hour angles. Typical upper limits were 0.1 K.

b) CO

Maps of the $J = 1 \rightarrow 0$ transitions of CO (115.3 GHz) and ^{13}CO (110.2 GHz) are shown in Figure 3, the CO map covering only the region north of OMC-2. The CO map shows a peak in the direction of OMC-2, in agreement with Gatley *et al.* (1974). The ^{13}CO emission does not peak in the direction of OMC-2, but rather in the center of the northern extension from OMC-2. The region of 2 mm H_2CO emission corresponds roughly to the 9 K contour on the ^{13}CO map.

The maps of the CO intensity at various velocities (Fig. 3) reveal emission peaks which are not discernible in the peak intensity maps. Most notable are the high-velocity peak (12–13 km s^{-1}) at (1950 coordinates) $5^h32^m50^s$, $-4°57'30''$ and the 10 km s^{-1} feature at $5^h31^m45^s$, $-4°57'30''$. Considerable velocity structure is also apparent in the profiles near this region (Fig. 4), as are rapid changes in the relative intensity of the CO and ^{13}CO. Also, the profiles of the two species often agree poorly. In particular, sudden line broadening, flat-topped profiles, and possible self-absorption may be seen at various positions. A striking feature of both CO maps is that the emission bends to the northwest at $\delta = -5°$ and then continues north. The photograph in Figure 5 shows that the cloud actually appears to bend around NGC 1977, the northern "star" in the sword of Orion. The emission drops precipitously at approximately the optical boundary of NGC 1977.

III. DISCUSSION

The presence of strong 2 mm formaldehyde emission undoubtedly indicates that a dense cloud connects OMC-1 and OMC-2, and then extends further to the north. In the following discussion, the molecular observations will be used to estimate the density and mass of the cloud. The velocity structure and its relationship to the rest of the Orion region will be discussed along with the interesting behavior in the vicinity of NGC 1977. Finally, we will use these observations to comment on the $^{13}C/^{12}C$ isotope abundance ratio.

a) Densities and Column Densities

One of the great advantages of studying H_2CO is that it provides a series of connected transitions whose excitation can be simultaneously studied. This is particularly true of the 2 mm and 2 cm lines, as discussed by Evans (1973) and Evans *et al.* (1975). For example, in the case of a uniform cloud, one can show that the optical depth, τ, of the 140 GHz line is given by

$$\tau\left[\frac{T_R(140.8)}{1 - e^{-\tau}} + 0.6\right] = 17.4\,\frac{T_R(14.4)}{1 - 2.7/T_x}, \qquad (1)$$

where $T_R(140)$ and $T_R(14.4)$ are the radiation temperatures of the 140 GHz and 14.4 GHz lines and T_x is the excitation temperature of the 14.4 GHz line. Though equation (1) applies to homogeneous clouds, it still serves as a qualitative guide to the optical depth of the 2 mm line.

Formaldehyde observations in the direction of OMC-1 have been extensively analyzed by Evans *et al.* (1975). From considerations which are equivalent to the use of equation (1), they concluded that the optical depth of the 2 mm line is probably at least 2. They further estimated the effects of trapping for the microturbulent and large-velocity-gradient case and arrived at a best estimate of the column density of ortho-H_2CO, $N_m \approx 2.2 \times 10^{14}$ cm^{-2}, and a molecular hydrogen density, $n_{H_2} \approx 10^5$ cm^{-3}.

In extending this analysis to the rest of the region, we note that the negative result for the 2 mm $H_2{}^{13}CO$ line northeast of OMC-1 implies an optical depth for the normal isotopic species lower than that toward OMC-1. The 2 cm observations suggest that the lower 2 mm optical depth persists over most of the cloud. Together with the lower kinetic temperature, compared with OMC-1, this implies that fairly high densities are required to produce the observed 2 mm emission.

To consider the situation in more detail, we first note that equation (1) requires $T_R(140) < 17.4T_R(14.4)$ if $T_x \gg 2.7$ K. Thus, for most of the positions studied at 2 cm, it appears that T_x is close to 2.7 K, regardless of the optical depth of the 2 mm line. However, as one increases τ, the interval of hydrogen density over which T_x is close to 2.7 K shifts to higher density and becomes smaller. For densities above and below this interval, 2 cm emission and absorption, respectively, are expected. With a knowledge of the collisional excitation rates one can use excitation calculations to see whether, for a given column density N_m, the interval of n_{H_2} allowed by the upper limits on the 2 cm lines will produce the observed 2 mm lines.

For low temperatures the calculations of Garrison *et al.* (1975) provide collision rates of sufficient accuracy. Trapping calculations were performed at 20 K and 30 K; collision rates at 20 K were supplied by Garrison (private communication), and rates at 30 K were obtained from these by scaling the downward

1976ApJ...209..452K

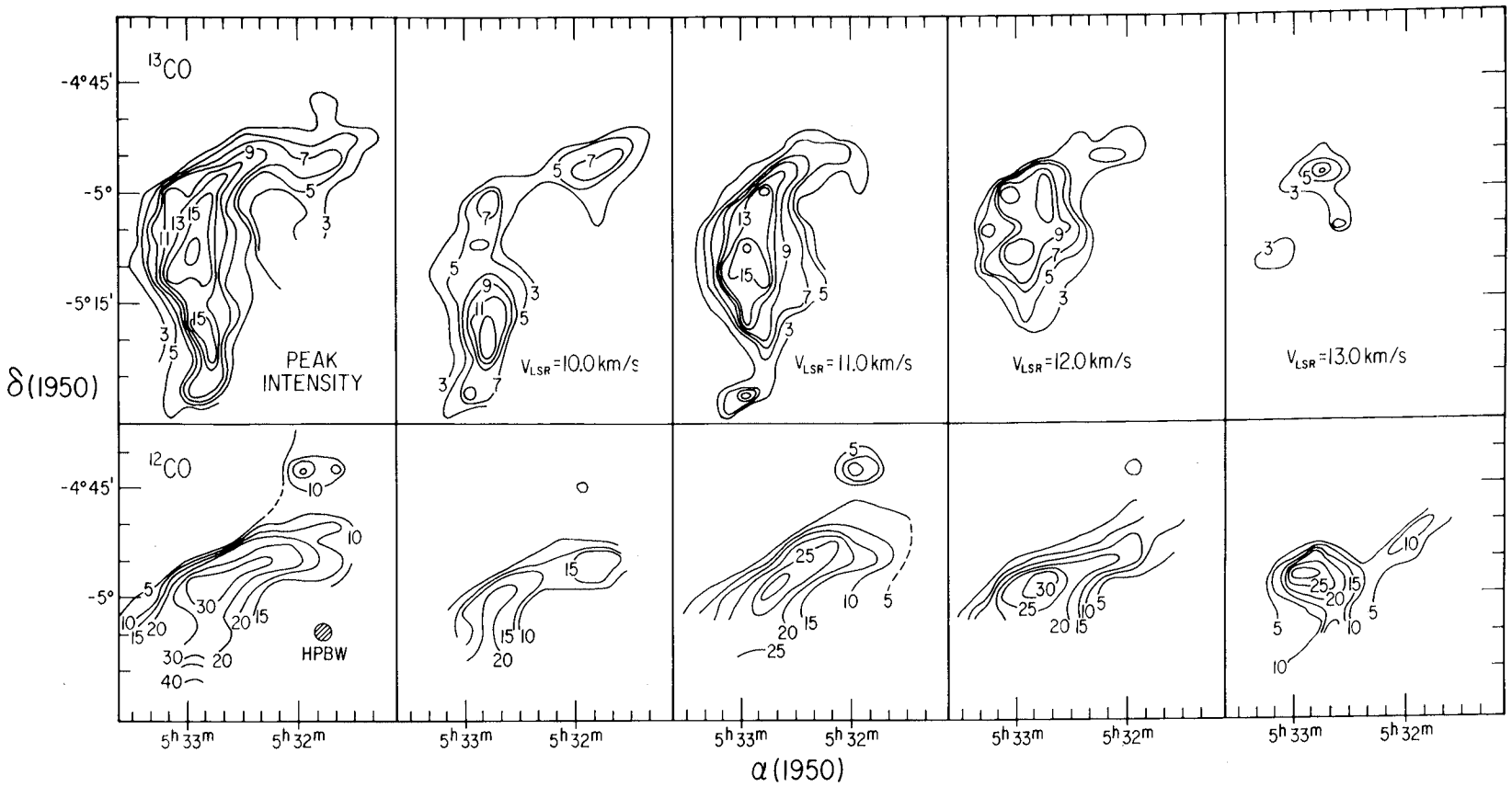

FIG. 3.—CO observations of the OMC-1/OMC-2 region. The upper row of maps represents contours of radiation temperature for $^{13}C^{16}O$, and the lower row, for $^{12}C^{16}O$. The maps were completely sampled at one beamwidth intervals (indicated by the shaded circle). For each isotope, the first map represents the peak radiation temperature at each position, while the following four maps show contours of radiation temperatures at four specific velocities.

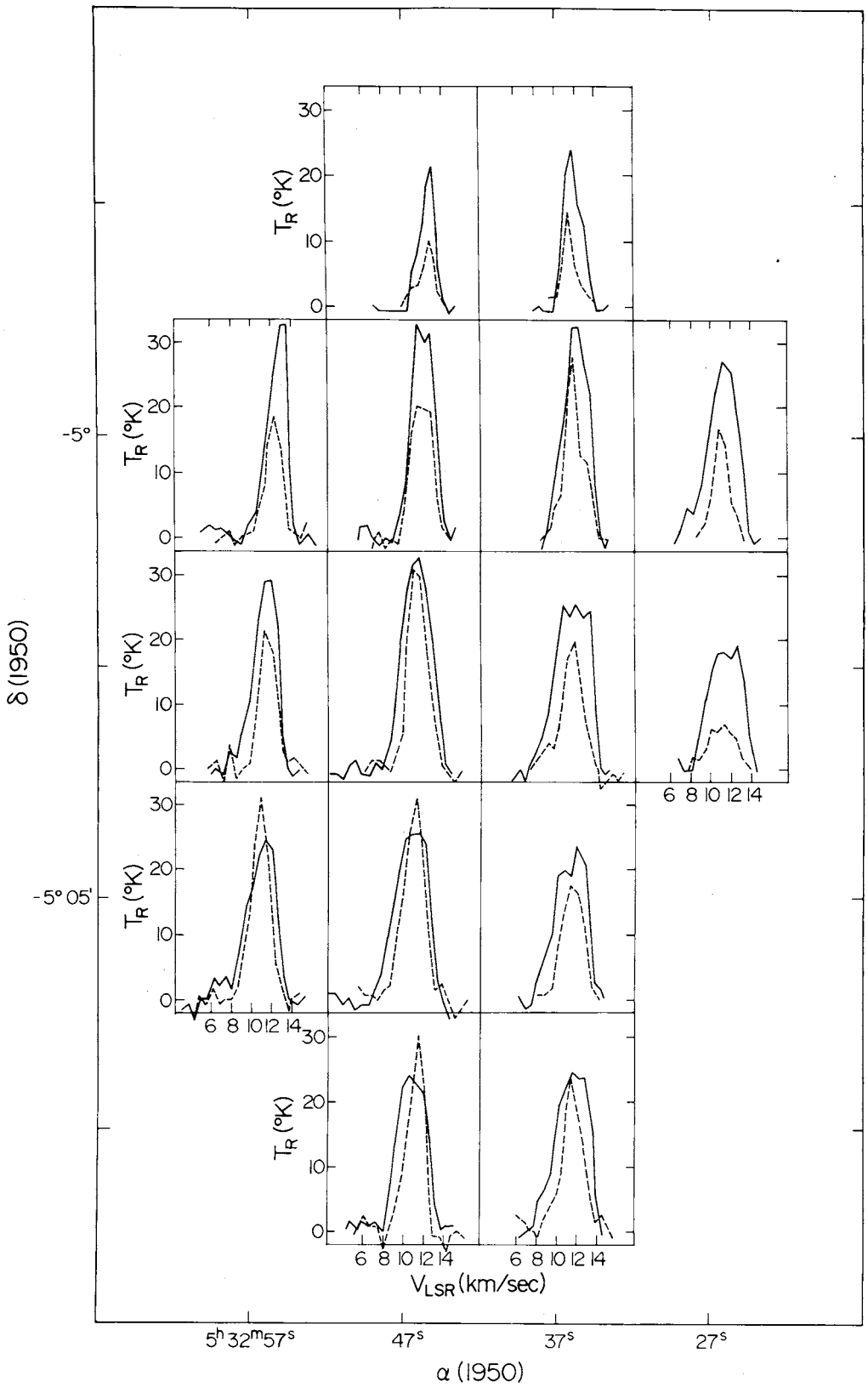

FIG. 4.—CO profiles in the vicinity of the CO peak near NGC 1977. The solid lines are the $^{12}C^{16}O$ spectra, and the dashed lines are the $^{13}C^{16}O$ spectra, with the intensities scaled up by a factor of 2.

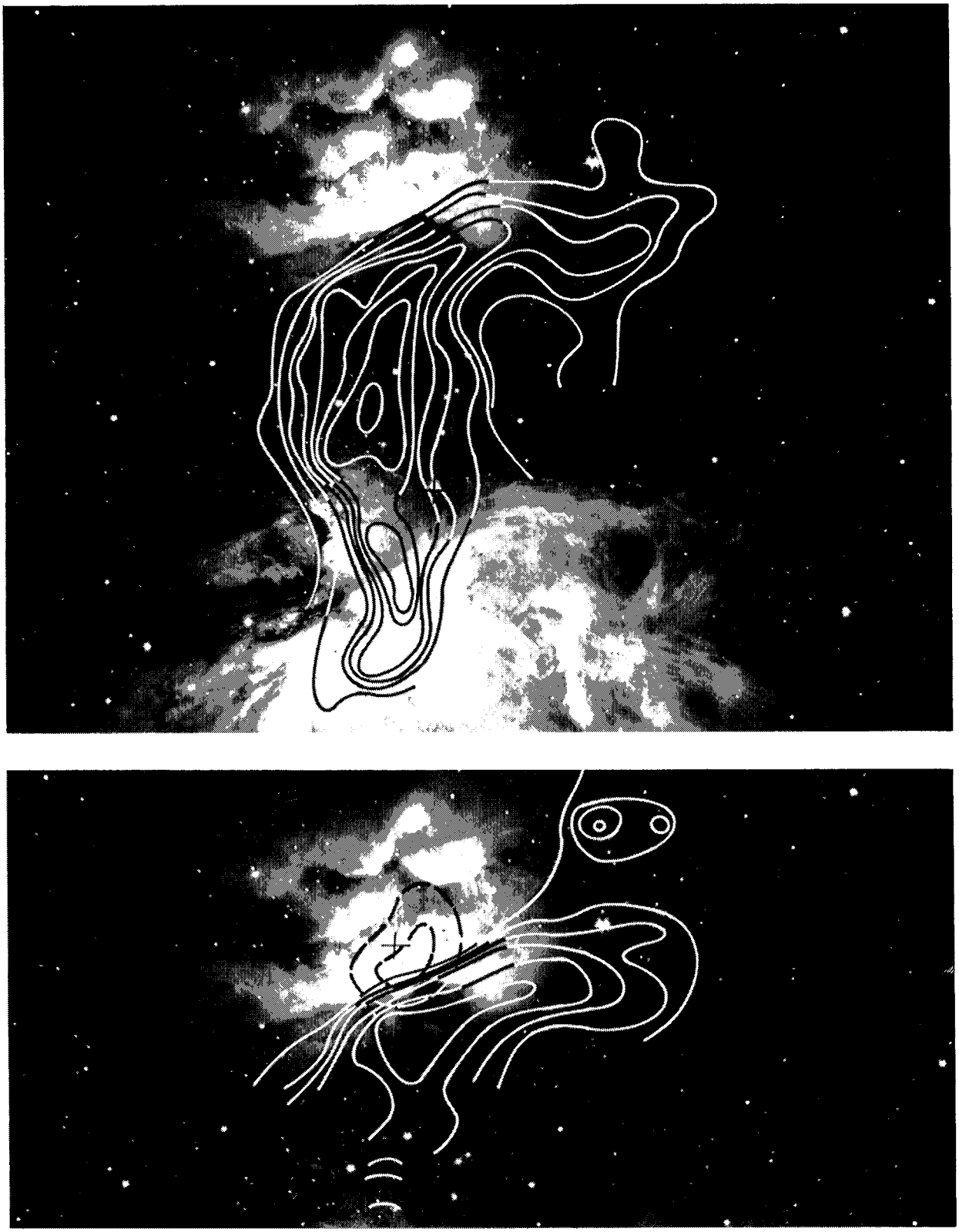

FIG. 5.—The $^{13}C^{16}O$ (*upper*) and $^{12}C^{16}O$ (*lower*) peak intensity contours from Fig. 3, superposed on a photograph showing Orion A and NGC 1977. The plus indicates the position of the exciting star for the H II region in NGC 1977. In the lower figure, the dotted lines represent the contours of 5 GHz emission (Goss and Shaver 1970).

rates by $\sqrt{T_k}$ and then deriving the upward rates from detailed balance. Because the cross sections show strong resonances, extrapolation to higher kinetic temperatures involves large uncertainties. Thus only positions with relatively low T_k can be analyzed this way.

A large-velocity-gradient model with spherical geometry was used, with $dv/dr = 1$ km s^{-1} pc^{-1}. At the optical depths involved, this should differ little from a microturbulent calculation. The results indicate that, for large N_m, the densities allowed by the 2 cm results were so high that the predicted 2 mm emission was stronger than observed. The highest N_m to produce reasonable results is 4×10^{13} cm^{-2}, for which $T_R(140) > 3$ K could be explained at $n_{H_2} \approx 10^5$ cm^{-3}. At half that column density, all the observed $T_R(140)$ could be explained by densities in the range (1–4) $\times$ 10^5 cm^{-3}. These results apply to positions from declinations $-5°09'$ to $-5°03'$, and to a lesser degree to positions up to $-4°57'$.

Below $-5°09'$, the kinetic temperatures become too high to use Garrison's rates, and the densities derived will depend strongly on the rates which determine T_x. It would be very hard to explain the 2 cm emission from OMC-1 with a simple extrapolation of Garrison's rates, since the large enhancement of $\sigma(1_{10}–3_{13})$ over $\sigma(1_{11}–3_{12})$ cools T_x even at high densities and temperatures. Indeed, this enhancement does decline as the collision energy increases (Garrison *et al.* 1975), suggesting that the cooling of T_x is less effective at high T_k. This may explain the prominence of 2 cm emission from OMC-1 compared with its striking absence in other, lower temperature sources (Evans *et al.* 1975) and over most of the dense cloud considered here. If we use the Model II cross sections of Evans *et al.* at $T_k =$ 60 K and $N_m = 1.2 \times 10^{14}$ cm^{-2}, the peak northeast of OMC-1 requires densities $\sim 10^5$ cm^{-3}, and OMC-2 requires $n_{H_2} \gtrsim 3 \times 10^4$ cm^{-3}. The region of weak 2 mm emission and relatively high T_k between OMC-1 and OMC-2 probably represents a density minimum with $n_{H_2} \approx 1 \times 10^4$ cm^{-3}; this region occurs at the declination of M43.

Because the densities appear to be high at least over the upper and lower third of the cloud, we adopt an average density of 5×10^4 cm^{-3} over the region where 2 mm emission is seen. If the line-of-sight dimension of the cloud is comparable to the width (i.e., it is cigar-shaped), this gives a total mass of 8×10^3 $M_\odot$. If the cloud is actually a disk seen edge-on, then the mass is a factor of 4 higher.

The mass can also be estimated from the CO observations. The ^{13}CO column density, N_{13}, is derived on the assumption that both isotopic species have the same excitation temperature. Despite the difficulties introduced by trapping in the optically thick CO (e.g., Goldreich and Kwan 1974), the H_2CO observations imply densities which are high enough to thermalize both species. If we assume a normal C to H abundance ratio, then the total column density of hydrogen in all forms is given by $N = N_{13}a/(3 \times 10^{-4}f)$, where a is the ^{12}C/^{13}C isotope abundance ratio and f is the fraction of all carbon in CO. We thus find that for the region covered by the ^{13}CO map, the total mass is $(2a/89f) \times 10^3$ $M_\odot$. If we take $a/89f = 3$ (Dickman 1975), then $M = 6 \times 10^3$ $M_\odot$, in excellent agreement with the mass obtained above on the assumption that the cloud is essentially prolate. Given the uncertainties in cloud models, such close agreement may be fortuitous, especially since Dickman's results are for lower density objects, and depletion of carbon onto the grains in the denser region could lower f, raising the mass.

b) Dynamics of the OMC-1–OMC-2 Region

To understand the structure of this region, it is useful to consider its relationship to the extended clouds in the Orion region. In a study of the large-scale distribution of CO in the Orion region, Kutner *et al.* (1976) find a velocity gradient for the extended (80 pc long) cloud L1641 of 0.135 km s^{-1} pc^{-1}, which is interpreted as a rotation with an angular velocity of at least 5.5×10^{-15} s^{-1}. The projection of the rotation axis is essentially east-west, with the northern end of the cloud rotating away from us. One would then expect that, as the cloud collapses, the denser parts will have a higher angular velocity. Indeed, Linke and Wannier (1974) find a gradient of 0.6 km s^{-1} pc^{-1} for a north-south strip of material within 30′ of the KL nebula.

The rotation pattern of the OMC-1/OMC-2 region is clearly shown by the results of the current study, combined with previous observations of H_2CO with a 1′ beam at 2 mm (Kutner 1972) and at 2 cm (Evans *et al.* 1976). These results are plotted in Figure 6, which shows the LSR velocity of various molecular lines as a function of declination for positions running along the center of the ridge. As expected, the pattern shows the largest velocity gradient for those regions which are presumed to have the highest densities, the KL molecular cloud and OMC-2. The continuous velocity change from KL to OMC-2 clearly establishes a direct relationship between these two condensations.

The density minimum between OMC-1 and OMC-2 seems contrary to the observation of a higher velocity gradient between OMC-1 and OMC-2 than north of OMC-2. We interpret this as evidence that the material has fragmented into two major sections, with part of the angular momentum going into the orbital motion of OMC-1 and OMC-2. The material between the two fragments, which has the same angular velocity as the orbital motion, is possibly just being dragged along by the orbiting bodies. There is also evidence that another fragment exists, since the 12–13 km s^{-1} CO peak at $\delta = -5°$ is separated from OMC-2 by approximately the OMC-1–OMC-2 distance, and its velocity difference from OMC-2 is the same as that of OMC-2 from KL. This would be consistent with some regular pattern of fragmentation.

c) NGC 1977

The emission nebula NGC 1977 is located almost directly north of the Orion Nebula, and is seen as the northern star in the sword. The optical nebula has a sharp boundary in the south. The 5 GHz survey of

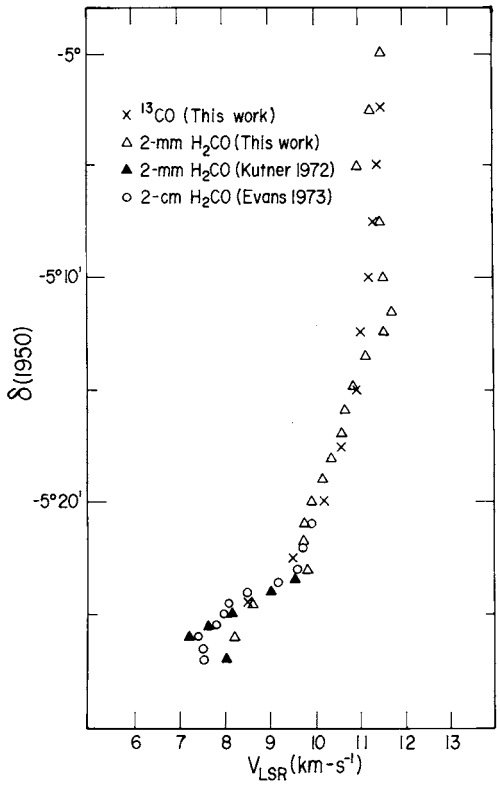

FIG. 6.—The velocity pattern of the OMC-1/OMC-2 region. The symbols represent the line-center velocities as a function of declination for positions along the center of the dense cloud.

Goss and Shaver (1970) reveals a small H II region in NGC 1977. As Figure 5 shows, the CO emission declines abruptly along the optical boundary, with the radiation temperature falling from 30 K to 5 K in about one beamwidth (2'.6).

The region around NGC 1977 may provide a graphic demonstration of the interaction between an H II region and the surrounding material. The 5 GHz continuum contours have been superposed on the photograph in Figure 5, showing that the boundary of the H II region agrees well with the observed CO boundary. Excitation of the H II region most likely comes from the B2 III star, HD 37018. If the H II region is ionization-bound and is expanding at 10 km s^{-1}, then the expansion age is about 5×10^4 yrs, in which case the exciting star may not have reached the main sequence. The star, however, is not centrally located with respect to the H II region. This would suggest that the H II region is density-bound in the northeast but is ionization-bound in the southwest, and is expanding in that direction. A shock front preceding the ionization front into the cloud may be responsible for the CO peak at 12–13 km s^{-1} at the northern end of the cloud. As Figure 5 shows, that peak occurs just at the edge of the outer continuum contour.

It appears that NGC 1977 has formed at the northern end of the molecular cloud, as the counterpart to the Orion Nebula at the southern end, as part of the pattern of fragmentation discussed above. Kutner and Thaddeus (1971) have shown that the molecular cloud must pass behind the Ori A H II region, and Zuckerman and Palmer (1974) have suggested that the rear of the H II region actually abuts the front of the molecular cloud. This is supported by the aperture synthesis map of the continuum radiation in Ori A (Gull and Martin 1975), which reveals a sharp boundary near the peak of the molecular cloud. The situation around NGC 1977 appears quite similar, but rotated through 90°, making the relationship between the H II region and the molecular cloud more apparent. By analogy with Ori A, recombination lines of carbon may be detectable from the interface between NGC 1977 and the molecular cloud.

d) Comments on the $H_2{}^{12}CO/H_2{}^{13}CO$ *Ratio*

The detection of the 137.4 GHz line of $H_2{}^{13}CO$ provides an excellent opportunity to investigate the carbon isotope ratio in Orion. It is useful to relate this line to the 14.4 GHz line of $H_2{}^{12}CO$ since both were observed with the same spatial resolution, and both are optically thin. This minimizes the uncertainties caused by source-structure and optical-depth effects. We take $T_R(137.4) = 0.2$ K. The antenna temperature at 14.4 GHz is 0.45 K; if the beam efficiency near transit is 0.5 for a 2' source, $T_R(14.4) = 0.9$ K. As noted above, the 137.4 GHz line of Wannier *et al.* has twice the width of ours, but both spectra are too noisy for an accurate determination of linewidth, and an average of the two profiles gives a linewidth consistent with the 14.4 GHz line. We note that if the 14.4 and 137.4 GHz emission come from the same region, then both lines are optically thin they should have the same linewidth, so we assume $\Delta v(137.4) = \Delta v(14.4)$.

From equation (4) of Evans *et al.* (1975), we have

$$\frac{N(H_2{}^{12}CO)}{N(H_2{}^{13}CO)} = 17.1 \frac{T_R(14.4)}{T_R(137.4)} \frac{X_{13}}{X_{12}}, \qquad (2)$$

where X_{13} is a function of the fractional populations in the two states connected by the transition observed in $H_2{}^{13}CO$ and X_{12} is the corresponding function for $H_2{}^{12}CO$. Since trapping will affect the fractional populations in $H_2{}^{12}CO$, the value of X_{13}/X_{12} will depend on the collision rates and the hydrogen and formaldehyde densities, but will generally increase with density. Excitation calculations for a wide range of parameters indicate that $X_{13}/X_{12} \geq 1$ for all reasonable cloud conditions. Substituting in equation (2) yields $H_2{}^{12}CO/H_2{}^{13}CO \geq 77$. For the most likely conditions in the extended cloud in OMC-1 (Evans *et al.* 1975), $X_{13}/X_{12} = 1.4$, raising the above ratio to 108. Since the source of 2 cm emission is more extended than Jupiter, we may have underestimated the beam efficiency, in which case these numbers can be lowered by at most 25 percent. There are calibration uncertainties of up to 20 percent in the 2 mm lines which will affect the final isotope ratio, but not the comparison of our analysis with that of Wannier *et al.*

From an observation of the 137.4 GHz line (whose intensity agrees with ours), Wannier *et al.* find a ratio

of 35 on the assumption that the 140 GHz line is optically thin. By the analysis of Evans *et al.* (1975), this assumption is inconsistent with the observed emission at 14.4 GHz. The above discussion gives some measure of the uncertainties which may arise in any oversimplification of the problem of line formation and source structure. Clearly, the calculations presented here also contain a number of assumptions, and further study is necessary. We believe that the presence of a number of connected transitions makes H_2CO an excellent molecule for studying the isotope problem, in a manner similar to that outlined above. However, many of the uncertainties can only be reduced by careful mapping and calibration of the 2 mm lines.

Our value for the H_2CO isotope ratio is in general agreement with that obtained from studies at 6 cm (Zuckerman *et al.* 1974; Evans *et al.* 1975), but differs significantly from the $^{12}CO/^{13}CO$ ratio deduced by Wannier *et al.* If fractionation effects on one or both molecules cannot account for the discrepancy (Watson *et al.* 1976), then a reexamination of the analysis employed is called for.

IV. CONCLUSIONS

These observations show a dense ($n_{H_2} \approx 5 \times 10^4$ cm^{-3}) molecular cloud connecting OMC-1 and OMC-2 and extending north of NGC 1977. The cloud is elongated north-south, with dimensions of 1.5 × 5 pc and a total mass of about $7 \times 10^3\ M_\odot$. Some extension of the cloud south of OMC-1 is indicated, and further observations are necessary to see if the dense cloud connecting OMC-1 and OMC-2 appears to run through the whole sword region.

The velocity pattern of the cloud is essentially one of rotation, and is consistent with this cloud having condensed out of the extended diffuse dust cloud L1641. A comparison of the density distribution and velocity pattern suggests that the cloud has fragmented, with much of the angular momentum going into the orbital motion of the densest subclouds. It appears likely that NGC 1977 is the northernmost fragment in this pattern.

The CO emission falls off very quickly at the edge of the H II region in NGC 1977. The relationship between the molecular cloud and the H II region is probably similar to that between the cloud and the Ori A H II region. The situation is more clearly shown for NGC 1977 because the H II region is to one side of the cloud, rather than in front of it. There is an extended CO peak close to the edge of the H II region, suggesting the possibility that a shock front preceding the ionization front is heating the gas.

One of us (M. L. K.) was partially supported by NASA grant NGR-33-008-191. Research in radio astronomy at the Owens Valley Radio Observatory is supported by the National Science Foundation under grant GP-30400-X1 and by the Office of Naval Research under contract N00014-67-A-0094-0019. N. J. E. also acknowledges support from NSF grant MPS 72-05070.

REFERENCES

Davis, J., and Vanden Bout, P. 1973, *Ap. Letters*, **15**, 43.
Dickman, R. L. 1975, *Ap. J.*, **202**, 50.
Evans, N. J., II. 1973, Ph.D. dissertation, University of California, Berkeley.
Evans, N. J., II, Zuckerman, B., Sato, T., and Morris, G. 1975, *Ap. J.*, **199**, 383.
Garrison, B. J., Lester, W. A., Jr., Miller, W. H., and Green, S. 1975, *Ap. J. (Letters)*, **200**, L175.
Gatley, I., Becklin, E. E., Matthews, K., Neugebauer, G., Penston, M. V., and Scoville, N. Z. 1974, *Ap. J. (Letters)*, **191**, L121.
Goldreich, P., and Kwan, J. 1974, *Ap. J.*, **189**, 441.
Goss, W. M., and Shaver, P. A. 1970, *Australian J. Phys., Suppl.* No. 14, p. 1.
Gull, S. F., and Martin, A. H. M. 1975, H II *Regions and Related Topics*, ed. T. L. Wilson and D. Downes (New York: Springer-Verlag).
Harvey, P. M., Gatley, I., Werner, M. W., Elias, J. H., Evans, N. J., II, Zuckerman, B., Morris, G., Sato, T., and Litvak, M. M. 1974, *Ap. J. (Letters)*, **189**, L87.
Kutner, M. L. 1972, Ph.D. dissertation, Columbia University.
Kutner, M. L., and Thaddeus, P. 1971, *Ap. J. (Letters)*, **168**, L67.
Kutner, M. L., Thaddeus, P., Penzias, A. A., Wilson, R. W., and Jefferts, K. B. 1973, *Ap. J. (Letters)*, **183**, L27.
Kutner, M. L., Tucker, K. D., Thaddeus, P., and Chin, G. 1976, in preparation.
Linke, R. A., and Wannier, P. G. 1974, *Ap. J. (Letters)*, **193**, L41.
Liszt, H. 1974, Ph.D. dissertation, Princeton University.
Lynds, B. T. 1962, *Ap. J. Suppl.* No. 64, **7**, 1.
Morris, M., Zuckerman, B., Turner, B. E., and Palmer, P. 1974, *Ap. J. (Letters)*, **192**, L27.
Thaddeus, P., Wilson, R. W., Kutner, M. L., Penzias, A. A., and Jefferts, K. B. 1971, *Ap. J. (Letters)*, **168**, L59.
Tucker, K. D., and Kutner, M. L. 1976, in preparation.
Turner, B. E., and Gammon, R. H. 1975, *Ap. J.*, **198**, 71.
Wannier, P. G., Penzias, A. A., Linke, R., and Wilson, R. W. 1976, *Ap. J.*, **204**, 26.
Watson, W. D., Anicich, V. G., and Huntress, W. T., Jr. 1976, *Ap. J. (Letters)*, **205**, L165.
Zuckerman, B., Buhl, D., Palmer, P., and Snyder, L. E. 1974, *Ap. J.*, **189**, 217.
Zuckerman, B., and Palmer, P. 1974, *Ann. Rev. Astr. and Ap.*, **12**, 279.

N. J. EVANS II: Department of Astronomy, University of Texas, Austin, TX 78712
M. L. KUTNER: Dept. of Physics, Rensselaer Polytechnic Institute, Troy, NY 12181
K. D. TUCKER: Department of Physics, Fordham University, Bronx, NY 10458